# Efficient optimization method for energy absorption capacity of origami structures

Cheng Xie
*Chongqing University; email: 18801017339@163.com*

Yongtao Bai
*Chongqing University; email: bai.yongtao@cqu.edu.cn*

ABSTRACT

As a geometric design method for creating arbitrary three-dimensional structures on two-dimensional flat materials based on specific crease patterns, origami's deployability and reconfigurable performance provide broad design and development space for mechanical metamaterials. This paper focuses on discovering the potential application value of origami structures in multistability and energy absorption from a theoretical perspective. Origami structures based on the triangulated cylinder patterns are considered to have both rigid folding and energy absorption capacity, but possibly affected by geometric features. To obtain the optimal geometric parameters contributed to the best energy absorption capacity, conventional finite element model is time-assuming, especially for structural optimization, while artificial intelligence proxy models are alternative choices. In this paper, one physics-informed neural network (PINN) based on the principle of virtual work is proposed to search for the optimal geometric parameters corresponding to the highest energy absorption capacity. Firstly, the key geometric characteristics of the triangulated origami corrugated column are found out, and then the rigid foldable kinematic properties of this kind of origami structure are obtained by analyzing the triangulated origami unit component. Based on the principle of minimum potential energy, the energy that can be absorbed in the process of deformation under this loading are obtained. Furthermore, with the key geometric parameters of this structure as the input layer and the maximum energy landscape as the optimization objective, a physically informed neural network is constructed. The results indicate that the network efficiently completes geometric parameter optimization for maximizing structural energy absorption, providing a structural design method for energy absorption optimization to create programmable and controllable smart structures further.

KEYWORDS: origami structures; energy absorption capacity; physics-informed neural networks; structural optimization

## 1. INTRODUCTION

Mechanical metamaterials are a kind of structural materials designed manually, which have excellent mechanical properties and unconventional physical properties, and have considerable application prospects in smart materials and structures. Among them, origami metamaterials originated from the mathematical exploration of origami art by scholars in the last century (Koryo 1985). Now, more and more scholars are focusing on the design of folding two-dimensional sheets (Klett et al. 2011) into three-dimensional origami structure to achieve specific mechanical properties in aerospace, machinery, architecture, medical health and other fields, such as tunable stiffness (Zhai et al. 2018; Tao et al. 2020), multistability (Silverberg et al. 2015; Bai et al. 2023) even programmable (Dudte et al. 2016; Zhang et al. 2022), negative Poisson ratio (Schenk et al. 2013), deformability (Miyazawa et al. 2022; Lee et al. 2017) and modularization (Neville et al. 2017; Janbaz et al. 2017). In essence, the shape-change of origami produces the above performance, so effective actuation is critical to required functionality. One way is to find the answers from nature, including fluid drive (Li et al. 2017) and bioinspired spring (Faber et al. 2018), inspired by hornbeam leaves (Mahadevan et al. 2005) and earwig wing. Other ways considering physics behavior includes magnetic control (Novelino et al. 2020), laser pressure method and thermal method at atomic-scale (Blees et al. 2015) and inflatable method at metre-scale (Melancon et al. 2021) to form the configurations of origami structures and the rotation of its hinges. Also, the findings of the linkage model for the origami of thick panels advance the application of origami structures in the real engineering (Chen et al. 2015).

Through the research on origami, how can we propose the advanced smart structure that could regulate its configuration as the external effects change? Firstly, field experiment needs to be done to reveal the real structure responses when external changes come (Kim et al. 2016). Then, the unit components of origami structures need to be determined, and the equivalent theoretical can be proposed and used to conduct the analysis on the foldability further (Frenzel et al. 2017). Finally, the energy landscape during the shape-change process of origami structures can be obtained, and the mechanical properties can be revealed subsequently.

Overvelde et al. (2017) presented the design strategy of complex origami structures. But now, artificial intelligence is considered to be able to accelerate the form optimization. In this paper, the triangulated origami column proved to have great energy absorption potential (Zhai et al. 2018) will be analyzed. Based on the principle of minimum potential energy (minPE), the energy landscapes of different origami columns with the geometry parameters change can be obtained, and through physics-informed neural network (PINN) model, efficient optimization method for energy absorption capacity of origami structures is proposed to realize the smart design.

## 2. ENERGY ANALYSIS ON ORIGAMI STRUCTURES

### 2.1. *Corrugated plate in civil engineering*

In the field of civil engineering, a kind of structure that can bear the loading during the normal service stage and the large deformation also under the impact or earthquake, is always expected. The corrugated plate, an original form of origami structures, has been used as the critical structural components to resist the large loading and large earthquake.

The application types of corrugated plate include corrugated plate steel column (CP-SC), corrugated plate shear wall (CP-SW) and flat-corrugated shear wall (FC-SW) etc. in civil engineering, such as culvert construction consisting of CP-SCs and seismic steel construction based on CP-SW or FC-SW. Above mentioned structures show both great load capacity and energy absorption capacity, due to high out-of-plane stiffness and deformability of corrugated plate.

Above applications of corrugated plates facilitate the subsequent research, that is the development of the more complex origami component, to realize the unity of load-bearing and energy-absorbing functions via tunable stiffness, which is considered as the smart structure.

(a) Culvert construction of CP-SCs

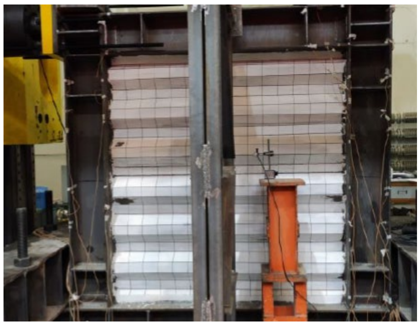

(b) Cyclic test of CP-SW (Xie et al. 2023)


(c) Cyclic test of FC-SW (Dou et al. 2023)

**Figure 1** Corrugated plate in civil engineering

## 2.2. *Geometry of new corrugated plate for origami column*

To obtain advanced smart structures switching between high load-bearing state and high energy absorption state, one kind of crease patterns varying with the geometry parameters change inspired by the triangulated cylinder (Guest et al. 1994) is studied. The geometry parameters of this crease pattern shown in Figure 2 consist of $\angle$CAB=$\alpha$, $\angle$ACB=$\beta$ and $l_{AB}$=$a$ of the triangular sheet ΔABC and the repeated number $n$ of ΔABC in the direction of rolling sheets into a column shape regarded as the unit component in Figure 3.

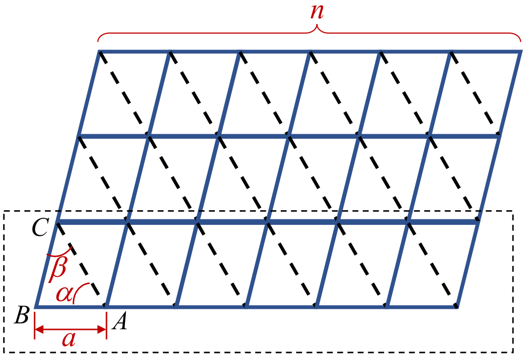


**Figure 2** Crease pattern of an origami column

As shown in Figure 3, this origami column unit (side length of polygon $l_{AB}$=$a$=1) can be deployed and folded when the height $h$ increases and decreases ($h$=0, folded completely), during which the top polygon rotates $\phi$ degrees around the center of its circumscribed circle while the bottom one is fixed. Noted that $r$ is the radius of the circumscribed circle, and the truss made by the fold lines of origami structures can substitute for rigid sheets in analysis (Yasuda et al. 2017).

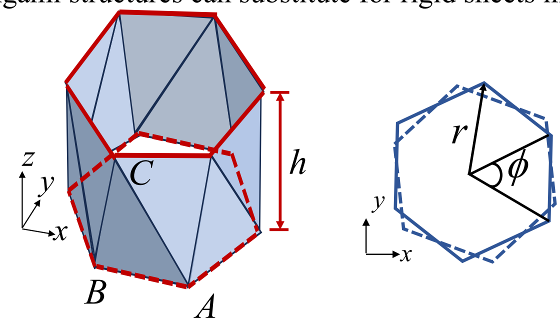


**Figure 3** A three-dimensional origami column unit and folding process

## 2.3. *Theoretical model of energy analysis*

During the deployment of the origami column unit, that is $h$ from 0 to the maximum value, the truss unit ΔABC shows the shape change, and the strains of the members AB, BC, AC occur naturally. Through the geometrical analysis on the shape-change of ΔABC, the strains of three members are obtained as *yipson_AB*, *yipson_BC* and *yipson_AC* in Eq. (1), (2), (3), respectively. Furthermore, from the energy view, almost all the energy generated by external action causing the collapse or deployment will be absorbed into the strain energy stored in the three members. The energy absorption $U$ of unit-length and unit-rigidity member can be calculated by Eq. (4).

$$yipson\_AB = 2\, r \sin\left(\frac{\pi}{n}\right) - 1 \tag{1}$$

$$yipson\_BC = \frac{\sin(\beta)\sqrt{h^2 - 2\cos(\phi)\, r^2 + 2\, r^2}}{\sin(\alpha)} - 1 \tag{2}$$

$$yipson\_AC = \frac{\sin(\beta)\sqrt{h^2 - 2\cos\left(\phi + \frac{2\pi}{n}\right) r^2 + 2\, r^2}}{\sin(\alpha + \beta)} - 1 \tag{3}$$

$$U = \frac{l_{AB}\; yipson\_AB^2 + l_{AC}\; yipson\_AC^2 + l_{BC}\; yipson\_BC^2}{2\,(l_{AB} + l_{AC} + l_{BC})} \tag{4}$$

Where, $l_{AB}=a=1$, according to the law of sines, $l_{BC}=a\cdot\sin\alpha / \sin\beta$, $l_{AC}=a\cdot\sin(\alpha+\beta) / \sin\beta$.

Given the two angles, α and β, and the repeated number $n$, the energy landscape of this origami column unit is determined. This means the energy absorption $U$ can be always known at each structural height $h$. But it hard to be calculated directly, due to the unknown top polygon rotation $\phi$ and radius $r$. Nevertheless, according to the principle of minimum potential energy, at any state of shape-change, the partial derivative of $U$ to $\phi$ and $U$ to $r$, namely, *dUdfi* and *dUdr*, are both equal to zero, as is calculated by Eq. (5) and (6), respectively. Also, the second partial derivative of $U$ to $\phi$ and $U$ to $r$ should be greater than zero. Besides, the partial derivative of $U$ to $h$ is calculated by Eq. (7), so that the maximum energy absorption during the shape-change process can be obtained. Therefore, theoretical model of energy analysis is built by Eq. (1)-(7).

$$dUdfi := \frac{\dfrac{2\, a\left(\dfrac{\sin(\beta)\sqrt{h^2 - 2\cos(\phi)\, r^2 + 2\, r^2}}{\sin(\alpha)} - 1\right)\sin(\phi)\, r^2}{\sqrt{h^2 - 2\cos(\phi)\, r^2 + 2\, r^2}} + \dfrac{2\, a\left(\dfrac{\sin(\beta)\sqrt{h^2 - 2\cos\left(\phi + \frac{2\pi}{n}\right) r^2 + 2\, r^2}}{\sin(\alpha+\beta)} - 1\right)\sin\left(\phi + \frac{2\pi}{n}\right) r^2}{\sqrt{h^2 - 2\cos\left(\phi + \frac{2\pi}{n}\right) r^2 + 2\, r^2}}}{2\left(a + \dfrac{a\sin(\alpha)}{\sin(\beta)} + \dfrac{a\sin(\alpha+\beta)}{\sin(\beta)}\right)} = 0 \tag{5}$$

$$dUdr := \frac{4\, a\left(2\, r\sin\left(\frac{\pi}{n}\right) - 1\right)\sin\left(\frac{\pi}{n}\right) + \dfrac{a\left(\dfrac{\sin(\beta)\sqrt{h^2 - 2\cos(\phi)\, r^2 + 2\, r^2}}{\sin(\alpha)} - 1\right)\left(-4\cos(\phi)\, r + 4\, r\right)}{\sqrt{h^2 - 2\cos(\phi)\, r^2 + 2\, r^2}} + \dfrac{a\left(\dfrac{\sin(\beta)\sqrt{h^2 - 2\cos\left(\phi + \frac{2\pi}{n}\right) r^2 + 2\, r^2}}{\sin(\alpha+\beta)} - 1\right)\left(-4\cos\left(\phi + \frac{2\pi}{n}\right) r + 4\, r\right)}{\sqrt{h^2 - 2\cos\left(\phi + \frac{2\pi}{n}\right) r^2 + 2\, r^2}}}{2\left(a + \dfrac{a\sin(\alpha)}{\sin(\beta)} + \dfrac{a\sin(\alpha+\beta)}{\sin(\beta)}\right)} = 0 \tag{6}$$

$$dUdh := \frac{\dfrac{2\, a\left(\dfrac{\sin(\beta)\sqrt{h^2 - 2\cos(\phi)\, r^2 + 2\, r^2}}{\sin(\alpha)} - 1\right) h}{\sqrt{h^2 - 2\cos(\phi)\, r^2 + 2\, r^2}} + \dfrac{2\, a\left(\dfrac{\sin(\beta)\sqrt{h^2 - 2\cos\left(\phi + \frac{2\pi}{n}\right) r^2 + 2\, r^2}}{\sin(\alpha+\beta)} - 1\right) h}{\sqrt{h^2 - 2\cos\left(\phi + \frac{2\pi}{n}\right) r^2 + 2\, r^2}}}{2\left(a + \dfrac{a\sin(\alpha)}{\sin(\beta)} + \dfrac{a\sin(\alpha+\beta)}{\sin(\beta)}\right)} = 0 \tag{7}$$

## 2.4. *Results and discussions*

Using the theoretical model of energy analysis, energy landscapes of origami columns with different α, β, and n are obtained. Considering the shape of column cross-section, n=4, 6 and 8 are used to form the quadrilateral, hexagon and octagon. The range of the angle α, β results from the limitation to make the ∠ABC be larger than 60 degree and the biggest angle of ΔABC.

The landscapes of above cases groups are shown in Figure 4, where the maximum energy during the height $h$ in the range of (0, 1) is marked by red solid point and recorded in Table 1, while the minimum green hollow point. For each group, as α+β>90 degree the landscapes are similar. When n=4, the maximum energy occurs at small angles with low height, while n=6 and n=8 at large angles with almost low height. Surprisingly, bistable states exist at special angles.

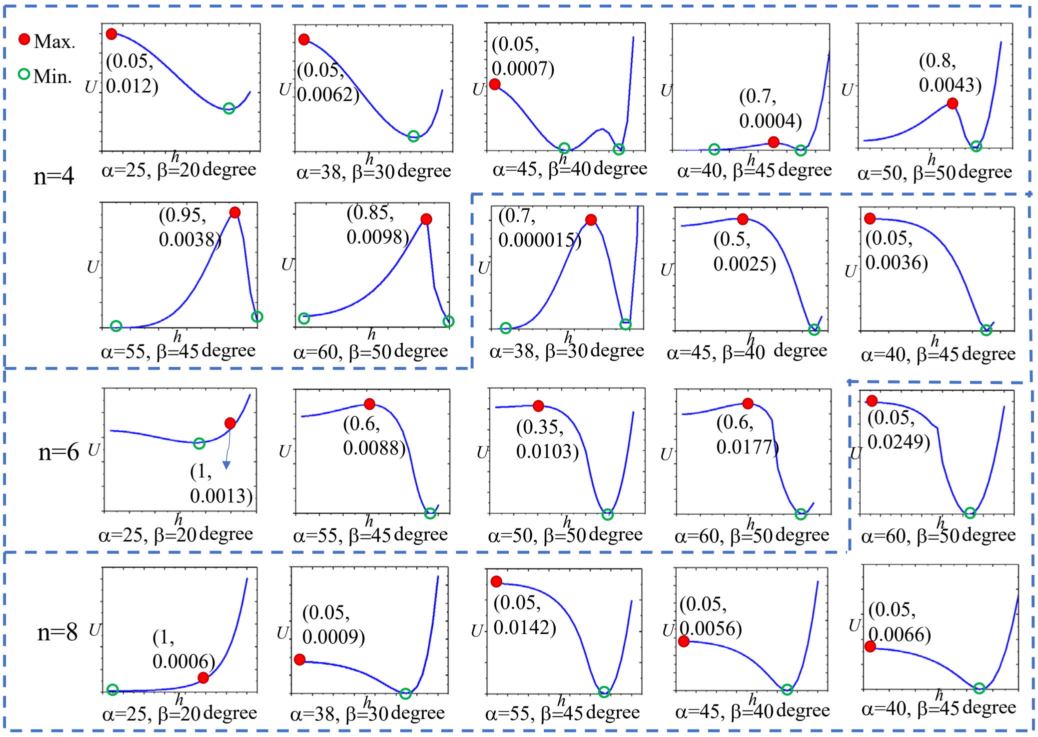


**Figure 4** Energy landscapes of origami columns with different α, β, and n

**Table 1** Cases of the maximum energy absorption and the corresponding shape

| α | β | $n$ | $h$ | $\phi$ | $r$ | $U_{Max}$ |
|---|---|---|---|---|---|---|
| 38 | 30 | 6 | 0.7 | 1.0631 | 0.9937 | 1.49E-05 |
| 25 | 20 | 6 | 1 | 0.8047 | 1.0509 | 0.001346 |
| 45 | 40 | 6 | 0.5 | 1.0530 | 0.9166 | 0.002503 |
| 40 | 45 | 6 | 0.05 | 0.9972 | 0.8986 | 0.003618 |
| 55 | 45 | 6 | 0.6 | 1.0726 | 0.8455 | 0.008772 |
| 60 | 50 | 6 | 0.6 | 1.0179 | 0.7862 | 0.017702 |
| 60 | 50 | 4 | 0.85 | 1.1545 | 0.5913 | 0.009828 |
| 55 | 45 | 4 | 0.95 | 0.8266 | 0.6460 | 0.003752 |
| 40 | 45 | 4 | 0.7 | 0.8317 | 0.6845 | 0.000439 |
| 45 | 40 | 4 | 0.05 | 1.6508 | 0.7461 | 0.000714 |
| 25 | 20 | 4 | 0.05 | 1.5804 | 0.8679 | 0.012164 |
| 25 | 20 | 8 | 1 | 0.6059 | 1.3476 | 0.000615 |
| 45 | 40 | 8 | 0.05 | 0.9120 | 1.1461 | 0.005648 |
| 40 | 45 | 8 | 0.05 | 0.7390 | 1.1405 | 0.006581 |
| 55 | 45 | 8 | 0.05 | 1.0114 | 1.0454 | 0.014165 |
| 60 | 50 | 8 | 0.05 | 1.0290 | 0.9586 | 0.024934 |
| 50 | 50 | 6 | 0.35 | 1.0607 | 0.8281 | 0.010344 |
| 50 | 50 | 4 | 0.8 | 0.7423 | 0.6412 | 0.004328 |
| 38 | 30 | 4 | 0.05 | 1.6669 | 0.8244 | 0.006197 |
| 38 | 30 | 8 | 0.05 | 1.0013 | 1.2415 | 0.000883 |

## 3. PINN-BASED LEARNING METHOD

To obtain the maximum energy $U_{Max}$ of the origami columns and the corresponding cross-section radius $r$, physics-informed neural network with particle swarm optimization (PSO-PINN) is built based on the accuracy of PSO in unimodal problems (Bai et al. 2024) and data-physical dual drive of PINN, as shown in Figure 5. The input layer includes five neurons, i.e., the angle α, β of the triangular cell, the repeated number $n$ in the rolling direction, the height $h$ from complete collapse to deployment, and the twist angle of the top polygon. The two neurons of the output layer are the maximum energy $U_{Max}$ and the raidus $r$ in the deployment process. PSO algorithm is applied to obtain the optimal initial values of weight and bias, i.e., {w1}{b1} between input layer and hidden layer, {w2}{b2} between hidden layer and output layer in Figure 5 through the smooth and continuous flight of particles in space. The basic hyperparameter setup of PSO algorithm is the same as that of the paper (Bai et al. 2024), including the data ratio 3:1 between the training sets and testing sets, except the seven neurons in the hidden layer. More importantly, aimed to improve the generalization capability only by the dataset from Table 1, performance function is the combination of the root mean squared error and the principle of minimum potential energy (minPE), represented as the expression of *Loss_value* in Eq. (8).

$$Loss\_value = \sqrt{\sum_{N=1}^{N_{\text{total}}} \left(U(N)_{\text{model}} - U(N)_{\text{real}}\right)^2 / N_{\text{total}}} + \sum_{N=1}^{N_{\text{total}}} \left|dUdr(N)\right| + \sum_{N=1}^{N_{\text{total}}} \left|dUdh(N)\right| \tag{8}$$

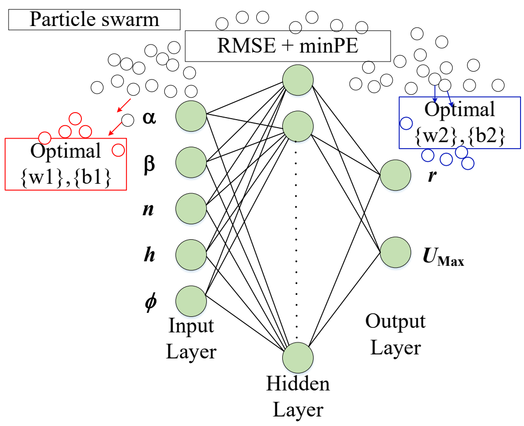


**Figure 5** Diagram of PSO-PINN model

The training results of the maximum energy $U_{Max}$ and the corresponding cross-section radius $r$ by PSO-PINN model are shown in Figure 6. It can be seen that the model and theoretical values of data points are close to the fitting curve Y=X. Also, the coefficients of determination R2 between them exceed 0.99, indicating that the model performance is very good. So, this trained PSO-PINN model can be used to predict the maximum energy $U_{Max}$ well.

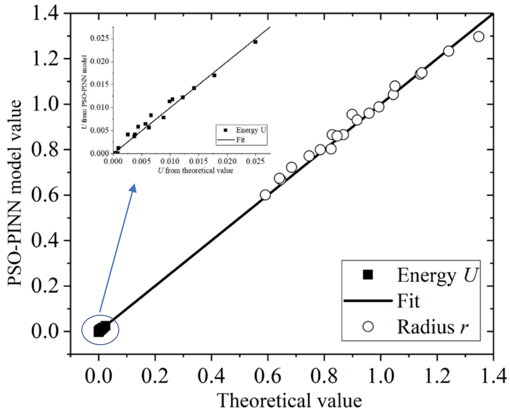

**Figure 6** The training results by PSO-PINN model

## 4. CONCLUSIONS

In this paper, the demand for next generation structural components is clarified firstly, to introduce the origami structures and its preliminary application at now. It was shown that after the success of the corrugated-plate component, the more complex origami components, considered to be used to form the smart structures i.e., the unity of load-bearing and energy-absorbing functions via tunable stiffness need to be studied further.

In this paper, based on the crease pattern via the repeated triangular cells, the wide range of the origami columns were analyzed from the energy view. First, the theoretical model of energy analysis is built by use of Eq. (1)-(7), according to the principle of minimum potential energy (minPE). Then, the groups of the energy landscapes were obtained, showing that bistable states exist at special angles and the locations of the maximum energy vary with the angle $\alpha$, $\beta$ of the triangular cell, and the repeated number n in the rolling direction. The largest normalized energy of above cases was 0.0249 from the origami column with $\alpha$=60 degree, $\beta$=50 degree and n=8 at height $h$=0.05$a$. Finally, the PSO-PINN model was proposed to predict the maximum energy $U_{\mathrm{Max}}$ efficiently based on the presentation of new equation of loss value, and would be used for the AI-based design of the smart structures in the future.

## ACKNOWLEDGEMENTS

This study was partially supported by the National Key R&D Program of China under Grant No. 2022YFB2602700, the National Natural Science Foundation of China (No. 52378216), the National Natural Science Foundation of China for Excellent Young Scientists Fund (Overseas), and the Fundamental Research Funds for the Central Universities (Grant No. 2022CDJKYJH052).

## REFERENCES

Bai, Y., Wang, S., Zhou, X., and Beer, M. 2023. Three-dimensional ori-kirigami metamaterials with multistability. *Physical Review E*, 107(3): 035004.

Bai, Y., Xie, C., and Zhou, X. 2024. AI-based macro model learning for high cycle fatigue assessment of welded joints in large-span steel structures. *International Journal of Fatigue*, 184: 108321.

Blees, M. K., Barnard, A. W., Rose, P. A., Roberts, S. P., McGill, K. L., Huang, P. Y., ... and McEuen, P. L. 2015. Graphene kirigami. *Nature*, 524(7564): 204-207.

Chen, Y., Peng, R., and You, Z. 2015. Origami of thick panels. *Science*, 349(6246): 396-400.

Dou, C., Xie, C., Wang, Y., and Yang, N. 2023. Cyclic loading test and lateral resistant behavior of flat-corrugated steel plate shear walls. *Journal of Building Engineering*, 66: 105831.

Dudte, L. H., Vouga, E., Tachi, T., and Mahadevan, L. 2016. Programming curvature using origami tessellations. *Nature materials*, 15(5): 583-588.

Faber, J. A., Arrieta, A. F., and Studart, A. R. 2018. Bioinspired spring origami. *Science*, 359(6382): 1386-1391.

Frenzel, T., Kadic, M., and Wegener, M. 2017. Three-dimensional mechanical metamaterials with a twist. *Science*, 358(6366): 1072-1074.

Guest, S.D., Pellegrino, S. 1994. The folding of triangulated cylinders. 1. Geometric considerations. *J Appl Mech*, 61:773–777.

Janbaz, S., Noordzij, N., Widyaratih, D. S., Hagen, C. W., Fratila-Apachitei, L. E., and Zadpoor, A. A. 2017. Origami lattices with free-form surface ornaments. *Science Advances*, 3(11):

eaao1595.
Kim, C.W., Chang, K.C., Kitauchi, S. and McGetrick, P.J. 2016. A field experiment on a steel Gerber-truss bridge for damage detection utilizing vehicle-induced vibrations, *Structural Health Monitoring*, 15(2): 174-192.
Klett, Y., Drechsler, K., Wang-Iverson, P., Lang, R. J., and Yim, M. 2011. Designing technical tessellations. In *Origami* (Vol. 5, No. ISBN 1568817142, pp. 305-322). CRC Press.
Koryo, M. 1985. Method of packaging and deployment of large membranes in space. *The Institute of Space and Astronautical Science report*, (618): 1-9.
Lee, D. Y., Kim, S. R., Kim, J. S., Park, J. J., and Cho, K. J. 2017. Origami wheel transformer: A variable-diameter wheel drive robot using an origami structure. *Soft robotics*, 4(2): 163-180.
Li, S., Vogt, D. M., Rus, D., and Wood, R. J. 2017. Fluid-driven origami-inspired artificial muscles. *Proceedings of the National Academy of Sciences*, 114(50): 13132-13137.
Mahadevan, L., Rica, S. 2005. Self-organized origami. *Science*, 307(5716): 1740-1740.
Melancon, D., Gorissen, B., García-Mora, C. J., Hoberman, C., and Bertoldi, K. 2021. Multistable inflatable origami structures at the metre scale. *Nature*, 592(7855): 545-550.
Miyazawa, Y., Chen, C. W., Chaunsali, R., Gormley, T. S., Yin, G., Theocharis, G., and Yang, J. 2022. Topological state transfer in Kresling origami. *Communications Materials*, 3(1): 62.
Neville, R. M., Chen, J., Guo, X., Zhang, F., Wang, W., Dobah, Y., ... and Peng, H. X. 2017. A Kirigami shape memory polymer honeycomb concept for deployment. *Smart Materials and Structures*, 26(5): 05LT03.
Novelino, L. S., Ze, Q., Wu, S., Paulino, G. H., and Zhao, R. 2020. Untethered control of functional origami microrobots with distributed actuation. *Proceedings of the National Academy of Sciences*, 117(39): 24096-24101.
Overvelde, J. T., Weaver, J. C., Hoberman, C., and Bertoldi, K. 2017. Rational design of reconfigurable prismatic architected materials. *Nature*, 541(7637): 347-352.
Schenk, M., and Guest, S. D. 2013. Geometry of Miura-folded metamaterials. *Proceedings of the National Academy of Sciences*, 110(9): 3276-3281.
Silverberg, J. L., Na, J. H., Evans, A. A., Liu, B., Hull, T. C., Santangelo, C. D., ... and Cohen, I. 2015. Origami structures with a critical transition to bistability arising from hidden degrees of freedom. *Nature materials*, 14(4): 389-393.
Tao, R., Ji, L., Li, Y., Wan, Z., Hu, W., Wu, W., ... and Fang, D. 2020. 4D printed origami metamaterials with tunable compression twist behavior and stress-strain curves. *Composites Part B: Engineering*, 201: 108344.
Xie, C., Dou, C., and Ru, Y. 2023. Cyclic test and lateral resistant design of corrugated plate shear walls. *Structures* Vol. 49: 748-764.
Yasuda, H., Tachi, T., Lee, M., and Yang, J. 2017. Origami-based tunable truss structures for non-volatile mechanical memory operation. *Nature communications*, 8(1): 962.
Zhang, X., Ma, J., Li, M., You, Z., Wang, X., Luo, Y., ... and Chen, Y. 2022. Kirigami-based metastructures with programmable multistability. *Proceedings of the National Academy of Sciences*, 119(11): e2117649119.
Zhai Z, Wang Y, Jiang H. 2018. Origami-inspired, on-demand deployable and collapsible mechanical metamaterials with tunable stiffness. *Proceedings of the National Academy of Sciences*, 115(9): 2032–2037.